HHS Public Access

Author manuscript

Cell Mol Neurobiol. Author manuscript; available in PMC 2023 January 01.

Published in final edited form as:

Cell Mol Neurobiol. 2022 January ; 42(1): 279–289. doi:10.1007/s10571-020-00880-9.

Serine Racemase Expression by Striatal Neurons

Shunsuke Takagi[1,2,3,4], **Matthew D. Puhl**[4], **Thea Anderson**[4], **Darrick T. Balu**[5,6], **Joseph T. Coyle**[4,5]

[1]Department of Psychiatry and Behavioral Sciences, Graduate School of Medical and Dental Sciences, Tokyo Medical and Dental University, 1-5-45 Yushima, Bunkyo-ku, Tokyo 113-8510, Japan

[2]Department of Psychiatry, Tokyo Medical and Dental University Hospital, 1-5-45 Yushima, Bunkyo-ku, Tokyo 113-8510, Japan

[3]Department of Neuropsychiatry, Graduate School of Medical Sciences, Kyushu University, 3-1-1 Maidashi, Higashi-ku, Fukuoka 812-8582, Japan

[4]Laboratory for Psychiatric and Molecular Neuroscience, McLean Hospital, 115 Mill Street, Belmont, MA 02478, USA

[5]Department of Psychiatry, Harvard Medical School, 25 Shattuck Street, Boston, MA 02115, USA

[6]Translational Psychiatry Laboratory, McLean Hospital, 115 Mill Street, Belmont, MA 02478, USA

Abstract

D-serine is synthesized by serine racemase (SR) and is a co-agonist at forebrain *N*-methyl-D-aspartate receptors (NMDARs). D-serine and SR are expressed primarily in neurons, but not in quiescent astrocytes. In this study, we examined the localization of D-serine and SR in the mouse striatum and the effects of genetically silencing SR expression in GABAergic interneurons (iSR−/−). iSR−/−mice had substantially reduced SR expression almost exclusively in striatum, but only exhibited marginal D-serine reduction. SR positive cells in the striatum showed strong co-localization with dopamine- and cyclic AMP-regulated neuronal phosphoprotein (DARPP32) in wild type mice. Transgenic fluorescent reporter mice for either the D1 or D2 dopamine receptors exhibited a 65:35 ratio for co-localization with D1 and D2 receptor positive cells, respectively. These results indicate that GABAergic medium spiny neurons receiving dopaminergic inputs in striatum robustly and uniformly express SR. In behavioral tests, iSR−/−mice showed a blunted response to the hedonic and stimulant effects of cocaine, without affecting anxiety-related behaviors. Because the cocaine effects have been shown in the constitutive SR−/−mice, the

✉Joseph T. Coyle joseph_coyle@hms.harvard.edu.

Author Contributions ST and JTC designed the study. DTB and JTC contributed to analysis and interpretation of data and assisted in the preparation of the manuscript. MDP and TA contributed to the histochemical studies and animal behavior testing. All authors had contributed to data collection and interpretation, and critically reviewed the manuscript. All authors approved the final version of the manuscript and agree to be accountable for all aspects of the work in ensuring that questions related to the accuracy or integrity of any part of the work are appropriately investigated and resolved.

Conflict of interest JTC reports consulting with Concert Pharm and holding a Patent on D-serine for the Treatment of Serious Mental Illness, which is owned by Massachusetts General Hospital. MDP is currently employed by Alkermes Pharm. DTB served as a Consultant for LifeSci Capital and received research support from Takeda Pharmaceuticals. ST and TA report no conflicts of interest.

Ethical Approval All animal procedures were conducted in accordance with the Guide for the Care and Use of Laboratory Animals (National Academy of Sciences, 2011) and were approved by the McLean Hospital Institutional Animal Care and Use Committee.

restriction of the blunted response to cocaine to iSR−/−mice reinforces the conclusion that D-serine in striatal GABAergic neurons plays an important role in mediating dopaminergic stimulant effects. Results in this study suggest that SR in striatal GABAergic neurons is synthesizing D-serine, not as a glutamatergic co-transmitter, but rather as an autocrine whereby the GABAergic neurons control the excitability of their NMDARs by determining the availability of the co-agonist, D-serine.

Keywords

D-serine; D-amino acid oxidase; Glutamic acid decarboxylase; Gamma-aminobutyric acid; *N*-methyl-D-aspartic acid; Serine racemase

Introduction

Since D-serine was discovered in the mammalian brain, it has emerged as an important *N*-methyl-D-aspartate receptor (NMDAR) co-agonist (Hashimoto et al. 1992). NMDARs consist of two GluN1 subunits that form an ion channel, usually blocked by a single magnesium (Mg^{2+}) ion, and two GluN2 subunits that bind glutamate. Receptor activation requires concurrent membrane depolarization to release the Mg^{2+} ion from the channel, glutamate binding to the GluN2 subunits, and either glycine or D-serine binding at the glycine modulatory site (GMS) on the GluN1 subunits. D-serine has three times higher binding affinity at GluN1 than glycine; so, D-serine is the primary endogenous co-agonist for forebrain NMDARs (Balu and Coyle 2015; Matsui et al. 1995).

D-serine is synthesized from L-serine by the cytosolic enzyme serine racemase (SR), a pyridoxal 5' phosphate (PLP) containing enzyme (Coyle et al. 2010; Nishikawa 2011). The reaction is reversible and requires Mg^{2+} and ATP as cofactors (Goto et al. 2009; Balu et al. 2014). SR-null mutant (*Srr*−/−) mice have brain D-serine levels 85–90% less than wild-type (WT) mice. The remaining D-serine most likely comes from diet or intestinal bacteria (Basu et al. 2009).

SR is enriched in cortico-limbic regions of the adult brain, whereas glycine appears to predominate in the cerebellum and brainstem. Because astrocytes produce the D-serine precursor, L-serine, and express its catabolic enzyme, D-amino acid oxidase (DAAO), SR was originally thought to be concentrated in glia (Mothet et al. 2005; Schell et al. 1995; Wolosker et al. 1999). Reactive astrocytes express SR (Balu et al. 2019; Perez et al. 2017), and cultured astrocytes begin expressing SR as they acquire the "reactive" or inflammatory phenotype (Li et al. 2018). But immunohistochemistry with *Srr*−/− mice as controls shows that under healthy physiological conditions, SR is expressed primarily by neurons (Miya et al. 2008; Ding et al. 2011; Ehmsen et al. 2013; Wolosker et al. 2016). These immunocytochemical findings were confirmed by conditionally silencing SR expression in a cell-specific fashion. By crossing *Srr*fl/fl mice with a Cre recombinase line driven by the promoter for glial fibrillary acidic protein (GFAP), SR expression in astrocytes would be expected to be suppressed; however, this astrocyte selective construct had no effect on the expression of SR in cortex. In contrast, crossing *Srr*fl/fl mice with a Cre recombinase line driven by the promoter for Ca^{2+}/calmodulin-dependent kinase II (CaMKII) eliminated SR in

cortico-limbic glutamatergic neurons, resulting in major reductions in SR expression (Balu et al. 2014; Balu and Coyle 2011). In the present study, we used mice with Cre recombinase driven by the promoter for glutamic acid decarboxylase-65 (GAD65; CreGAD2) to silence *Srr*fl/fl expression in GABAergic neurons. In this report, we have focused primarily on the impact of silencing SR expression in striatal GABAergic neurons.

Methods

Animals

WT, constitutive *Srr*−/− , and selective neuronal *Srr*−/− (nSR−/−) or astrocytic SR−/− (aSR−/−) mice were bred as previously described, by crossing SRfl/fl mice with Cre recombinase lines driven by either a CaMKII neuronal promoter or a glial fibrillary acidic protein (GFAP) astrocytic promoter (Basu et al. 2009; Benneyworth et al. 2012). We bred SR+/− parents to produce WT and SR−/− siblings and used SRfl/fl mice as controls against their iSR−/−, nSR−/− and aSR−/− littermates. All mice were backcrossed at least ten generations onto a C57BL/6J background.

Glutamic acid decarboxylase synthesizes the inhibitory neurotransmitter γ-aminobutyric acid (GABA) by decarboxylating glutamate. It has a 65-kDa isoform (GAD65; GAD2) and a 67-kDa isoform (GAD67; GAD1), produced by two distinct GABAergic populations. GAD2 mCherry mice which have a transgenic fluorescent protein driven by the promoters for the gene (Peron et al. 2015) were obtained from the Jackson Laboratory. A GAD2 Cre recombinase line [Gad2tm2(cre), Jackson Laboratories, Bar Harbor, ME] was bred with *srr*fl/fl mice to selectively remove SR from GAD65-expressing interneurons (iSR−/−).

Striatal inhibitory neurons can also be classified by their dopamine receptor expression. To examine SR expression in D1 direct projections and D2 indirect projections, we obtained D1- and D2-tdTomato mice, which have fluorescent transgenes driven by the promoters for either D1 or D2 dopamine receptors (Thibault et al. 2013); kindly provided by Michael Benneyworth, PhD, University of Minnesota). Three-month-old mice were used for experiments on adults. Animals were housed in a temperature- and humidity-controlled facility (22 °C) on 12 h light/dark cycles with food and water ad libitum. All animal procedures were approved by the McLean Hospital Institutional Animal Care and Use Committee.

Western Blotting

The striatum was dissected for immunoblotting, as previously described (Balu and Coyle 2011), with goat anti SR (1:500; Santa Cruz Biotechnology, Santa Cruz, CA), an antibody validated against *Srr*−/− mice (Wolosker et al. 2016; Takagi et al. 2015). β-Actin was a loading control. Antiserum (goat polyclonal) against D-amino acid oxidase (DAAO) was purchased from Abcam (ab34697).

High-Performance Liquid Chromatography (HPLC)

As previously described (Benneyworth et al. 2012), the striatum was dissected and homogenized, then the protein concentration was adjusted to 1 mg/mL and 4 mM/g L-

homocysteic acid was added as an internal standard. Proteins were precipitated from the samples by centrifuging in 5% trichloroacetic acid for 30 min at 18,000 × *g* in 4 °C; and then washing three times with water-saturated diethyl ether.

Amino acids were derivatized with *o*-phthaldialdehyde (Alfa Aesar, Ward Hill, MA) and *N-tert*-butyloxycarbonyl-L-cysteine (Novabiochem, Gibbstown, NJ) as previously described (Benneyworth et al. 2012), and concentrations were calculated by normalizing each internal standard to a standard sample run that morning. The HPLC system used consists of an SCL-10A controller, two LC-10AT VP pumps, an SIL-10AD auto injector, a DGU-20A5 degasser and an RF-551 fluorescence monitor (all from Shimadzu Corporation, Kyoto, Japan).

Immunohistochemistry and Immunofluorescence

SR-expressing neurons were counted on immune-histochemically stained 20-μm sections from SRfl/fl and iSR−/− mice after transcardially perfusing them with 0.1 M phosphate-buffered saline (PBS) and 4% paraformaldehyde. As previously described (Balu et al. 2014), the sections were incubated ~40 h at 4 °C with mouse anti SR (1:2000, BD Biosciences, San Jose, CA) diluted in PBS with 3.0% bovine serum albumin and 0.1% Triton X-100 followed by 90 min in a biotinylated horse anti-mouse secondary antibody (1:1000, Vector Laboratories; Burlingame, CA). The immunocomplexes were stained with 3,3-diaminobenzidine (DAB) using ABC Elite reagents (Vector Laboratories) according to manufacturers' instructions. Experimental and control samples were processed in parallel.

Dual immunofluorescent staining was used to determine which subpopulations of striatal neurons expressed SR. Slices were incubated overnight at room temperature with SR anti-goat (1:100, Santa Cruz) along with either mouse anti-DARPP-32 (1:2000, Santa Cruz), mouse anti-CamKII (1:500, Abcam), mouse anti-GAD67 (1:100, Millipore, Billerica, MA), goat anti-choline acetyl transferase (ChAT) (1:500, Millipore) or mouse anti-parvalbumin (1:1000, Sigma-Aldrich, St. Louis, MO) followed by Alexa Fluor secondary antibodies. Contrast and brightness of immunofluorescent images in the figures were adjusted in PowerPoint 2011 (Microsoft, Redmond, WA).

SR co-localization with D1 and D2 dopamine receptors was calculated using the Optical Fractionator module of Stereo Investigator (MBF Bioscience, Williston, VT). The chosen grid sizes (500 μm^2 in striatum; 650 μm^2 in nucleus accumbens) and counting frame (120 μm^2) estimated densities with high precision (coefficient of error <0.09). Three sections per region spanning the rostral-caudal axis according to Paxinos and Franklin (2001) were counted from three mice and balanced by hemisphere.

Behavioral Testing

Elevated Plus Maze—The elevated plus maze consisted of four arms elevated 80 cm above the floor. Each arm (12 cm wide, 76 cm long) was joined to the others by a central square (12 cm × 12 cm) in a cross-like disposition. A wall (30 cm in height) enclosed two opposite arms, while the other two arms were open. Placing the mouse on the platform facing an open arm started the test. During the next 10 min the number of entries in open

or closed-arms and the time spent in open or closed-arms was recorded. The mice were considered to have entered an arm when all four limbs were located in an arm of the maze. All sessions were video recorded by a camera mounted above the maze and analyzed in real-time using EthoVision XT software (version 7.1; Noldus Information Technology, Leesburg, VA). The percentage of time the mice spent in the open arms and the percentage of entries into open arms were calculated.

Open Field Test—Spontaneous locomotor activity and habituation to a novel open field environment were assessed using clear Plexiglas® chambers fitted with three 16-beam I/R arrays and placed inside sound-attenuating cubicles (ENV-510 System, Med Associates, Inc., St. Albans, VT, USA). Photobeam breaks were recorded and translated into locomotor activity using open field activity software (Activity Monitor 5.0, Med Associates, Inc.) The center zone was defined using the coordinates (4.5, 12; 12, 12; 4.5, 4.5; 12, 4.5) of the 16 × 16 cm chamber. The experiment time was 600 s. The distance moved by mice and the duration of time spent in the center zone were recorded.

Place Conditioning Test—Place conditioning was conducted in four identical acrylic chambers (30 cm × 15 cm × 15 cm), as previously described (Smith et al. 2014). Chamber floors consisted of inter-changeable halves with distinct textures (hole or grid). Hole floors were made from perforated 16-gauge stainless steel mounted on acrylic rails with 6.4-mm round holes placed at 9.5-mm staggered centers. Grid floors were made from 2.3-mm stainless steel rods mounted on acrylic rails 6.4 mm apart. All place-conditioning sessions were video recorded and analyzed in real-time using EthoVision XT software.

Place-conditioning procedures were conducted, as previously described (Smith et al. 2014; Bechtholt et al. 2004; Cunningham 1995; Cunningham et al. 1999) in the apparatus described above. Specifically, animals were randomly assigned to GRID+or GRID- conditioning groups, with genotype (SRfl/fl, i*Srr*−/−) counterbalanced. Conditioning consisted of five phases, as follows: habituation, conditioning, preference testing, and extinction (Fig. 2). Prior to each session, animals were transported from the colony room to the place-conditioning room where they were allowed to habituate for 1 h. Lighting was dimmed (~ 10 1×). On day 1 (habituation), all animals received injections (i.p.; injection volume 10 ml/kg) of 0.9% bacteriostatic saline and were immediately placed in the conditioning chambers on a smooth Plexiglas floor with white matting beneath it for 30 min. On days 2 and 3 (conditioning), animals received injections (i.p.; injection volume 10 ml/kg) of saline in the morning and cocaine (20 mg/kg) in the afternoon (4 h later) and were immediately placed in the conditioning chambers for 30 min. GRID+animals were placed on the hole side for saline injections and on the grid side for cocaine injections, whereas GRID-animals were placed on the grid side for saline injections and on the hole side for cocaine injections. On day 4 (preference testing), all animals received injections (i.p.; injection volume 10 ml/kg) of 0.9% bacteriostatic saline and were immediately placed in the conditioning chambers with access to both the grid and hole sides for 30 min. Days 5–7 (extinction) were identical to day 4 (preference testing).

Intracranial Self-stimulation (ICSS)—ICSS procedures were performed as previously described (Puhl et al. 2019). The mice (approximately 2 months old) were anesthetized (i.p.,

ketamine 80 mg/kg and xylazine 10 mg/kg), and monopolar-stimulating electrodes were stereotactically implanted in the medial forebrain bundle (in mm from bregma, anterior–posterior: – 1.9, mediolateral: – 1.0, dorsal-ventral: – 5.0 below dura, according to the atlas of Paxinos and Franklin 2001). Following ICSS electrode implantation surgery, the animals were individually housed and allowed a 1-week recovery period. Thereafter, all mice were trained to respond for brain stimulation by spinning an operant wheel during daily 1-h sessions over the course of 2–4 weeks (Muschamp et al. 2012). Stimulation frequency was fixed at 141 Hz, and stimulation current was adjusted to the lowest value that would support stable responding (i.e. one quarter wheel turn, which translated to one brain stimulation reward, per second). After identifying this minimum current for each mouse, the current was held constant during subsequent training sessions, where the mice were allowed to respond to 15 stimulation frequencies presented in descending order (0.05 $\log_{10}$ unit steps) during fifteen 50-s trials. Each trial was preceded by a 5-s priming period, during which noncontingent stimulation was given at the frequency used for that trial. Also, each trial was followed by a 5-s timeout period, during which responding was not reinforced. Responding was recorded during each 50-s trial in each set of 15 trials (termed a “pass”). The range of frequencies was adjusted over the course of training for 4–6 weeks, so that the mice responded through the highest six to seven frequencies stably over six passes (90 min of training). The lowest frequency that supported responding (ICSS threshold or T0) was computed with least-squares line of best-fit analysis (Carlezon and Chartoff 2007). When the animals were observed to have stable mean ICSS thresholds (< 10% variability over three consecutive days), the effects of vehicle and different doses of cocaine (3, 6, 12 mg/kg) on ICSS threshold were determined. The mice responded through three passes immediately before drug treatment, and thresholds from the second and third passes were averaged to obtain the baseline (ICSS threshold and maximal response rate) parameters. Each mouse then received either vehicle or cocaine (3, 6, 12 mg/kg) and was tested for three passes. The mice were treated with vehicle or each dose of cocaine twice, in ascending then descending order, with a minimum of 2 days between treatments.

Statistical Analyses

The results of western blotting, HPLC, elevated plus maze, place preference and open field test were compared using unpaired Student *t*-test. Mixed factorial and one-way analysis of variance (ANOVA) tests were conducted for ICSS. These analyses were done with the GraphPad PRISM software (version 7.03, GraphPad Software, Inc., La Jolla, CA) Values of $p < 0.05$ were considered statistically significant.

Results

iSrr−/− Mice Have Reduced SR Expression in Striatum Without a Corresponding Reduction in d-serine

To examine the role of SR in striatal inhibitory neurons (Balu et al. 2014), we selectively silenced the *Srr* gene in GAD65-expressing interneurons and measured the resulting changes in protein expression and D-serine concentrations. We found significant SR protein decreases in striatum ($p = 0.015$) and modest effects on hippocampal and cortical SR in adult mice (Fig. 1a–c).

We found approximately 70% fewer SR-expressing cells in striatum and 65% fewer in the nucleus accumbens of iSR−/− mice than in the SRfl/fl controls (Fig. 1h–i). We found nearly the same reductions in nSR−/− mice in the nucleus accumbens (Fig. 2). It should be emphasized that nSR construct silences SR expression only in cells that express CamKII. This finding indicates that the GAD65 cells targeted in our iSR−/− mice account for nearly all CamKII expressing neurons in these regions, which we confirmed by co-staining SRlf/fl striatal slices for SR and CamKII. In both the immunohistochemical and immunofluorescence studies, no SR expression was observed in glia.

We used HPLC to measure the D-serine concentrations in the same samples and observed only a small and statistically insignificant reduction in D-serine in striatum ($p = 0.140$) and other areas (Fig. 3a–c). This finding is perplexing given the large reduction in SR, but a similar result was previously observed in nSR−/− mice, which showed consistent strong reductions in SR protein but a much smaller reduction in D-serine levels (Benneyworth et al. 2012). We measured striatal expression of DAAO, an astrocytic protein that catabolizes D-serine, to determine whether iSR−/− mice maintained D-serine homeostasis by decreasing DAAO expression. However, DAAO protein levels in iSR−/− mice were not affected (Fig. 3d).

Medium Spiny Neurons Express Striatal SR; Cholinergic and Parvalbumin Expressing Neurons Do Not

Approximately 95% of striatal neurons are medium spiny neurons (MSN), identifiable by dopamine- and cAMP-regulated neuronal phosphoprotein 32 (DARPP32) expression (Kemp and Powell 1971; Ouimet et al. 1984, 1998). We observed strong co-localization of SR with DARPP32 (Fig. 4a–c). The striatum has a small but densely branching population of cholinergic interneurons, identifiable by ChAT expression (Phelps and Vaughn 1986; Dautan et al. 2014), These striatal cholinergic neurons do not co-express SR (Fig. 4d). The striatum also contains a population of isolated fast-spiking interneurons that express parvalbumin. These interneurons also do not co-express SR (Fig. 4e).

Association of SR Expression with Dopamine Receptors

MSN’s have two distinct subtypes distinguished by the dopamine receptor subtype expressed and their projection patterns. D1-receptor-expressing neurons project directly to basal ganglia output nuclei, whereas D2-receptor-expressing neurons project indirectly by way of the globus pallidus and sub-thalamic nuclei (Soares-Cunha et al. 2016; Surmeier et al. 2007). We stained for SR in D1R and D2R-tdTomato expressing mice, and found that ~ 66% of striatal SR cells expressed D1R and that ~ 37% expressed D2R (Table 1).

iSR−/− Mice Showed Impaired Sensitization to Cocaine

Constitutive SR−/− have shown a blunted response to the hedonic and stimulant effects of cocaine (Puhl et al. 2019), as well as elevated basal extracellular levels of glutamate and dopamine with blunted responses to cocaine in the ventral striatum. Consistent with these results, the iSR−/− mice showed significantly less cocaine locomotor sensitization than SRfl/fl mice (Fig. 5e; $p = 0.010$) and did not maintain a preference for the cocaine chamber

on extinction days in place conditioning test, whereas the SRfl/fl controls did not extinguish (Fig. 5e–g).

In the ICSS experiment, a consistent result was also obtained (Fig. 5h, i). Mice were implanted with ICSS electrodes and trained to respond to electrical stimulation (see Methods section). Upon reaching the stability criteria for ICSS responding, the mice received cocaine treatment. ICSS thresholds and maximum response rates were analyzed by using repeated measures ANOVAs varying genotype (SRfl/fl or iSR−/−) and cocaine dose (0, 3, 6 or 12 mg/kg). For ICSS thresholds, significant main effects of cocaine dose ($F = 46.756$, $p < 2e\text{-}16$) and genotype ($F = 3.803$, $p = 0.05$) were found. In the dose response study, an unpaired t-test showed a significant genotype difference at the 12 mg/kg dose ($p = 0.0222$), but not at the lower doses. This result suggests that iSR−/− mice react less in ICSS threshold following cocaine administration, consistent with previous results (Puhl et al. 2019). These results suggest that striatal GAD65 interneurons synthesize the D-serine involved in the hedonic response to cocaine.

Discussion

The striatum receives cholinergic innervation from interneurons and brainstem sources (e.g. latero-dorsal tegmental area, pedunculopontine nuclei) and GABAergic innervation from striatal MSNs (Kita 1993; Dautan et al. 2014). The MSNs in turn project directly to the *substantia nigra* or indirectly to the *substantia nigra* via the *globus pallidus.* Additionally, the striatum receives dopaminergic projections from the ventral tegmental area (VTA) and the substantia nigra (SNr) and glutamatergic inputs from several areas, including the cortex, hippocampus, amygdala, and thalamus (Swanson 1982; Phillipson and Griffiths 1985; Finch 1996; Groenewegen et al. 1999; Britt et al. 2012). These glutamatergic inputs synapse onto the heads of dendritic spines of the striatal GABAergic MSNs, whereas dopaminergic inputs make synapses *en-passage* onto the spine neck, allowing for an important and complex interaction between these two inputs in the modulation of MSN activity (Freund et al. 1984; Xu et al. 1989).

Miya et al. (2008) first described the expression of SR in GABAergic MSNs in the striatum. They reported that the SR immunoreactivity was primarily localized to the perikarya and the shafts of the dendrites. Our study confirms the universal expression of SR in the striatal MSNs including the 65% that express dopamine D2 receptors and project to the *substantia nigra* and the 35% that express dopamine D1 and project to the *globus pallidus.* In contrast, we found that a sub-population of fast-firing PV-expressing GABAergic interneurons in the striatum, which modulate the activity of MSNs (Lee et al. 2017), do not express SR. PV-expressing GABAergic neurons in the amygdala, an extension of the striatum, also did not express SR (Balu et al. 2018). In contrast, D-serine was co-localized with a substantial but variable portion of cortical and hippocampal PV-expressing interneurons (Balu et al. 2014), thus suggesting that co-localization of PV and SR is not uniform across brain regions. In addition, the striatal cholinergic interneurons do not express SR.

These observations of SR expression in subpopulations of GABAergic neurons raise the question about the function of D-serine in inhibitory neurons. Obviously, D-serine is not

a “co-transmitter” with GABA as the post-synaptic GABAA receptors do not have a glycine modulatory site. A more parsimonious explanation is that D-serine is serving as a coagonist at the NMDARs on the GABAergic dendrites post-synaptic to glutamatergic afferents. Further undermining the role of D-serine as a co-transmitter is the evidence that it is not released by Ca^{2+}-dependent exocytotic mechanisms but rather facilitated transport, likely by AscT-1 (Sason et al. 2017). While the evidence supports an autocrine role for D-serine synthesized in the striatal MSNs, this finding does not preclude a potential role for facilitated release of D-serine from striatal glutamatergic afferents innervating the MSNs.

The recent tissue culture study of cerebral cortex by Lynch’s laboratory elegantly demonstrated the clumping of SR immunoreactivity around the post-synaptic density in dendrites under the VGut-expressing glutamatergic terminals on both glutamatergic and GABAergic neurons (Lin et al. 2016). This distribution of SR is consistent with the original description by Miya et al. (2008) of SR having a predominant dendritic localization in striatal MSNs. Our recent research has demonstrated that SR expression is dynamically regulated with increased expression in circumstances associated with increased glutamatergic neurotransmission (Balu et al. 2018). This regulation of the SR expression by glutamatergic neurotransmission is consistent with a post-synaptic localization of SR.

Our recent in vivo dialysis study revealed a striking and significant elevation of basal dopamine release in the ventral striatum and a blunted response to a cocaine challenge (Puhl et al. 2019). This finding is consistent with a disinhibition of dopaminergic neurons in the *substantia nigra* and VTA. Given the major GABAergic innervation of the dopaminergic perikarya and proximal dendrites (Bolam and Smith 1990), reduced GABAergic inhibitory drive due to impaired glutamatergic neurotransmission resulting from deficient function of NMDA receptors could account for the increased dopamine release in the striatum. This finding suggests that pharmacologically enhancing NMDA receptor function could counter-intuitively reduce dopaminergic disinhibition. Pharmacologic and gene knock-out studies support this hypothesis that enhanced NMDA receptor function is associated with increased locomotor sensitization with stimulants and ICSS (Benneyworth and Coyle 2012; Puhl et al. 2015; Areal et al. 2019).

In summary, SR is robustly expressed in striatal GABAergic neurons post-synaptic to a diffuse glutamatergic input from the cerebral cortex and other structures. The localization of SR to dendrites and, more specifically, within the post-synaptic density adjacent to glutamatergic terminal boutons suggests that SR is synthesizing D-serine not as a glutamatergic co-transmitter but rather as an autocrine, whereby the GABAergic neurons control the excitability of their own post-synaptic NMDA receptors by determining the availability of the co-agonist, D-serine. These GABAergic NMDA receptors appear to modulate the locomotor sensitization associated with repeated exposure to stimulants and ICSS.

Acknowledgements

We thank Dr. Toru Nishikawa and Dr. Makoto Taniguchi for advice and support, as well as Alexandra Berg and Kendall Presti for animal colony maintenance and genotyping. This research was supported by A Phyllis and Jerome Lyle Rappaport Mental Health Research Scholars Award, 1K99MH099252-01A1, and 5R00MH099252-04

(DTB); R01MH05190 and P50MH0G0450 (JTC). Shunsuke Takagi was supported in part by Strategic Young Researcher Overseas Visits Program for Accelerating Brain Circulation from the Japan Society for the Promotion of Science (S2301). Since participating in this study, MDP has taken a position at Alkermes.

References

Areal LB, Hamilton A, Martins-Silva C, Pires RGW, Ferguson SSG (2019) Neuronal scaffolding protein spinophilin is integral for cocaine-induced behavioral sensitization and ERK1/2 activation. Mol Brain 12(1):15. 10.1186/s13041-019-0434-7 [PubMed: 30803445]

Balu DT, Coyle JT (2011) Neuroplasticity signaling pathways linked to the pathophysiology of schizophrenia. Neurosci Biobehav Rev 35(3):848–870. 10.1016/j.neubiorev.2010.10.005 [PubMed: 20951727]

Balu DT, Coyle JT (2015) The NMDA receptor 'glycine modulatory site' in schizophrenia: D-serine, glycine, and beyond. Curr Opin Pharmacol 20C:109–115. 10.1016/j.coph.2014.12.004

Balu DT, Pantazopoulos H, Huang CCY, Muszynski K, Harvey TL, Uno Y, Rorabaugh JM, Galloway CR, Botz-Zapp C, Berretta S, Weinshenker D, Coyle JT (2019) Neurotoxic astrocytes express the D-serine synthesizing enzyme, serine racemase, in Alzheimer's disease. Neurobiol Dis 130:104511. 10.1016/j.nbd.2019.104511 [PubMed: 31212068]

Balu DT, Presti KT, Huang CCY, Muszynski K, Radzishevsky I, Wolosker H, Guffanti G, Ressler KJ, Coyle JT (2018) Serine racemase and D-serine in the amygdala are dynamically involved in fear learning. Biol Psychiatry 83(3):273–283. 10.1016/j.biopsych.2017.08.012 [PubMed: 29025687]

Balu DT, Takagi S, Puhl MD, Benneyworth MA, Coyle JT (2014) D-serine and serine racemase are localized to neurons in the adult mouse and human forebrain. Cell Mol Neurobiol 34(3):419–435. 10.1007/s10571-014-0027-z [PubMed: 24436034]

Basu AC, Tsai GE, Ma CL, Ehmsen JT, Mustafa AK, Han L, Jiang ZI, Benneyworth MA, Froimowitz MP, Lange N, Snyder SH, Bergeron R, Coyle JT (2009) Targeted disruption of serine racemase affects glutamatergic neurotransmission and behavior. Mol Psychiatry 14(7):719–727. 10.1038/mp.2008.130 [PubMed: 19065142]

Bechtholt AJ, Smith R, Raber J, Cunningham CL (2004) Enhanced ethanol-, but not cocaine-induced, conditioned place preference in Apoe(−/−) mice. Pharmacol Biochem Behav 77(4):783–792. 10.1016/j.pbb.2004.02.002 [PubMed: 15099924]

Benneyworth MA, Coyle JT (2012) Altered acquisition and extinction of amphetamine-paired context conditioning in genetic mouse models of altered NMDA receptor function. Neuropsychopharmacology 37(11):2496–2504. 10.1038/npp.2012.108 [PubMed: 22763616]

Benneyworth MA, Li Y, Basu AC, Bolshakov VY, Coyle JT (2012) Cell selective conditional null mutations of serine racemase demonstrate a predominate localization in cortical glutamatergic neurons. Cell Mol Neurobiol 32(4):613–624. 10.1007/s10571-012-9808-4 [PubMed: 22362148]

Bolam JP, Smith Y (1990) The GABA and substance P input to dopaminergic neurones in the substantia nigra of the rat. Brain Res 529(1–2):57–78 [PubMed: 1704287]

Britt JP, Benaliouad F, McDevitt RA, Stuber GD, Wise RA, Bonci A (2012) Synaptic and behavioral profile of multiple glutamatergic inputs to the nucleus accumbens. Neuron 76(4):790–803. 10.1016/j.neuron.2012.09.040 [PubMed: 23177963]

Carlezon WA Jr, Chartoff EH (2007) Intracranial self-stimulation (ICSS) in rodents to study the neurobiology of motivation. Nat Protoc 2(11):2987–2995. 10.1038/nprot.2007.441 [PubMed: 18007634]

Coyle JT, Balu D, Benneyworth M, Basu A, Roseman A (2010) Beyond the dopamine receptor: novel therapeutic targets for treating schizophrenia. Dialogues Clin Neurosci 12(3):359–382 [PubMed: 20954431]

Cunningham CL (1995) Localization of genes influencing ethanol- induced conditioned place preference and locomotor activity in BXD recombinant inbred mice. Psychopharmacology 120(1):28–41. 10.1007/bf02246142 [PubMed: 7480533]

Cunningham CL, Dickinson SD, Grahame NJ, Okorn DM, McMullin CS (1999) Genetic differences in cocaine-induced conditioned place preference in mice depend on conditioning trial duration. Psychopharmacology 146(1):73–80. 10.1007/s002130051090 [PubMed: 10485967]

Dautan D, Huerta-Ocampo I, Witten IB, Deisseroth K, Bolam JP, Gerdjikov T, Mena-Segovia J (2014) A major external source of cholinergic innervation of the striatum and nucleus accumbens originates in the brainstem. J Neurosci 34(13):4509–4518. 10.1523/JNEUROSCI.5071-13.2014 [PubMed: 24671996]

Ding X, Ma N, Nagahama M, Yamada K, Semba R (2011) Localization of D-serine and serine racemase in neurons and neuroglias in mouse brain. Neurol Sci 32(2):263–267. 10.1007/s10072-010-0422-2 [PubMed: 20890627]

Ehmsen JT, Ma TM, Sason H, Rosenberg D, Ogo T, Furuya S, Snyder SH, Wolosker H (2013) D-serine in glia and neurons derives from 3-phosphoglycerate dehydrogenase. J Neurosci 33(30):12464–12469. 10.1523/JNEUROSCI.4914-12.2013 [PubMed: 23884950]

Finch DM (1996) Neurophysiology of converging synaptic inputs from the rat prefrontal cortex, amygdala, midline thalamus, and hippocampal formation onto single neurons of the caudate/putamen and nucleus accumbens. Hippocampus 6(5):495–512. 10.1002/(SICI)1098-1063(1996)6:5<495:AID-HIPO3>3.0.CO;2-I [PubMed: 8953303]

Freund TF, Powell JF, Smith AD (1984) Tyrosine hydroxylase-immunoreactive boutons in synaptic contact with identified striatonigral neurons, with particular reference to dendritic spines. Neuroscience 13(4):1189–1215 [PubMed: 6152036]

Goto M, Yamauchi T, Kamiya N, Miyahara I, Yoshimura T, Mihara H, Kurihara T, Hirotsu K, Esaki N (2009) Crystal structure of a homolog of mammalian serine racemase from *Schizosaccharomyces pombe*. J Biol Chem 284(38):25944–25952. 10.1074/jbc.M109.010470 [PubMed: 19640845]

Groenewegen HJ, Wright CI, Beijer AV, Voorn P (1999) Convergence and segregation of ventral striatal inputs and outputs. Ann N Y Acad Sci 877:49–63 [PubMed: 10415642]

Hashimoto A, Nishikawa T, Hayashi T, Fujii N, Harada K, Oka T, Takahashi K (1992) The presence of free D-serine in rat brain. FEBS Lett 296(1):33–36 [PubMed: 1730289]

Kemp JM, Powell TP (1971) The connexions of the striatum and globus pallidus: synthesis and speculation. Philos Trans R Soc Lond B 262(845):441–457 [PubMed: 4399123]

Kita H (1993) GABAergic circuits of the striatum. Prog Brain Res 99:51–72 [PubMed: 8108557]

Lee K, Holley SM, Shobe JL, Chong NC, Cepeda C, Levine MS, Masmanidis SC (2017) Parvalbumin interneurons modulate striatal output and enhance performance during associative learning. Neuron 93(6):1451–1463.e1454. 10.1016/j.neuron.2017.02.033 [PubMed: 28334608]

Li S, Uno Y, Rudolph U, Cobb J, Liu J, Anderson T, Levy D, Balu DT, Coyle JT (2018) Astrocytes in primary cultures express serine racemase, synthesize D-serine and acquire A1 reactive astrocyte features. Biochem Pharmacol 151:245–251. 10.1016/j.bcp.2017.12.023 [PubMed: 29305854]

Lin H, Jacobi AA, Anderson SA, Lynch DR (2016) D-serine and serine racemase are associated with PSD-95 and glutamatergic synapse stability. Front Cell Neurosci 10:34. 10.3389/fncel.2016.00034 [PubMed: 26941605]

Matsui T, Sekiguchi M, Hashimoto A, Tomita U, Nishikawa T, Wada K (1995) Functional comparison of D-serine and glycine in rodents: the effect on cloned NMDA receptors and the extracellular concentration. J Neurochem 65(1):454–458 [PubMed: 7790891]

Miya K, Inoue R, Takata Y, Abe M, Natsume R, Sakimura K, Hongou K, Miyawaki T, Mori H (2008) Serine racemase is predominantly localized in neurons in mouse brain. J Comp Neurol 510(6):641–654. 10.1002/cne.21822 [PubMed: 18698599]

Mothet JP, Pollegioni L, Ouanounou G, Martineau M, Fossier P, Baux G (2005) Glutamate receptor activation triggers a calcium-dependent and SNARE protein-dependent release of the gliotransmitter D-serine. Proc Natl Acad Sci USA 102(15):5606–5611. 10.1073/pnas.0408483102 [PubMed: 15800046]

Muschamp JW, Nemeth CL, Robison AJ, Nestler EJ, Carlezon WA Jr (2012) DeltaFosB enhances the rewarding effects of cocaine while reducing the pro-depressive effects of the kappa-opioid receptor agonist U50488. Biol Psychiatry 71(1):44–50. 10.1016/j.biopsych.2011.08.011 [PubMed: 21962331]

Nishikawa T (2011) Analysis of free D-serine in mammals and its biological relevance. J Chromatogr B 879(29):3169–3183. 10.1016/j.jchromb.2011.08.030

Ouimet CC, Langley-Gullion KC, Greengard P (1998) Quantitative immunocytochemistry of DARPP-32-expressing neurons in the rat caudatoputamen. Brain Res 808(1):8–12 [PubMed: 9795103]

Ouimet CC, Miller PE, Hemmings HC Jr, Walaas SI, Greengard P (1984) DARPP-32, a dopamine- and adenosine 3':5'-monophosphate-regulated phosphoprotein enriched in dopamine-innervated brain regions. III. Immunocytochemical localization. J Neurosci 4(1): 111–124 [PubMed: 6319625]

Paxinos G, Franklin KBJ (2001) The mouse brain in stereotaxic coordinates, 2nd edn. Academic, San Diego

Perez EJ, Tapanes SA, Loris ZB, Balu DT, Sick TJ, Coyle JT, Liebl DJ (2017) Enhanced astrocytic D-serine underlies synaptic damage after traumatic brain injury. J Clin Investig 127(8):3114–3125. 10.1172/JCI92300 [PubMed: 28714867]

Peron SP, Freeman J, Iyer V, Guo C, Svoboda K (2015) A cellular resolution map of barrel cortex activity during tactile behavior. Neuron 86(3):783–799. 10.1016/j.neuron.2015.03.027 [PubMed: 25913859]

Phelps PE, Vaughn JE (1986) Immunocytochemical localization of choline acetyltransferase in rat ventral striatum: a light and electron microscopic study. J Neurocytol 15(5):595–617 [PubMed: 3534148]

Phillipson OT, Griffiths AC (1985) The topographic order of inputs to nucleus accumbens in the rat. Neuroscience 16(2):275–296 [PubMed: 4080159]

Puhl MD, Berg AR, Bechtholt AJ, Coyle JT (2015) Availability of *N*-methyl-D-aspartate receptor coagonists affects cocaine-induced conditioned place preference and locomotor sensitization: implications for comorbid schizophrenia and substance abuse. J Pharmacol Exp Ther 353(3):465–470. 10.1124/jpet.115.223099 [PubMed: 25788713]

Puhl MD, Desai RI, Takagi S, Presti KT, Doyle MR, Donahue RJ, Landino SM, Bergman J, Carlezon WA Jr, Coyle JT (2019) *N*-methyl-D-aspartate receptor co-agonist availability affects behavioral and neurochemical responses to cocaine: insights into comorbid schizophrenia and substance abuse. Addict Biol 24(1):40–50. 10.1111/adb.12577 [PubMed: 29168271]

Sason H, Billard JM, Smith GP, Safory H, Neame S, Kaplan E, Rosenberg D, Zubedat S, Foltyn VN, Christoffersen CT, Bundgaard C, Thomsen C, Avital A, Christensen KV, Wolosker H (2017) Asc-1 transporter regulation of synaptic activity via the tonic release of D-serine in the forebrain. Cereb Cortex 27(2): 1573–1587. 10.1093/cercor/bhv350 [PubMed: 26796213]

Schell MJ, Molliver ME, Snyder SH (1995) D-serine, an endogenous synaptic modulator: localization to astrocytes and glutamate-stimulated release. Proc Natl Acad Sci USA 92(9):3948–3952 [PubMed: 7732010]

Smith KL, John CS, Sypek EI, Ongur D, Cohen BM, Barry SM, Bechtholt AJ (2014) Exploring the role of central astrocytic glutamate uptake in ethanol reward in mice. Alcohol Clin Exp Res 38(5): 1307–1314. https://doi.org/10.llll/acer.12361 [PubMed: 24655029]

Soares-Cunha C, Coimbra B, Sousa N, Rodrigues AJ (2016) Reappraising striatal D1- and D2- neurons in reward and aversion. Neurosci Biobehav Rev 68:370–386. 10.1016/j.neubiorev.2016.05.021 [PubMed: 27235078]

Surmeier DJ, Ding J, Day M, Wang Z, Shen W (2007) D1 and D2 dopamine-receptor modulation of striatal glutamatergic signaling in striatal medium spiny neurons. Trends Neurosci 30(5):228–235. 10.1016/j.tins.2007.03.008 [PubMed: 17408758]

Swanson LW (1982) The projections of the ventral tegmental area and adjacent regions: a combined fluorescent retrograde tracer and immunofluorescence study in the rat. Brain Res Bull 9(1–6):321–353 [PubMed: 6816390]

Takagi S, Balu DT, Coyle JT (2015) Subchronic pharmacological and chronic genetic NMDA receptor hypofunction differentially regulate the Akt signaling pathway and Arc expression in juvenile and adult mice. Schizophr Res 162(1–3):216–221. 10.1016/j.schres.2014.12.034 [PubMed: 25592804]

Thibault D, Loustalot F, Fortin GM, Bourque MJ, Trudeau LE (2013) Evaluation of D1 and D2 dopamine receptor segregation in the developing striatum using BAC transgenic mice. PLoS ONE 8(7):e67219. 10.1371/journal.pone.0067219 [PubMed: 23843993]

Wolosker H, Balu DT, Coyle JT (2016) The rise and fall of the D-serine-mediated gliotransmission hypothesis. Trends Neurosci 39(11):712–721. 10.1016/j.tins.2016.09.007 [PubMed: 27742076]

Wolosker H, Blackshaw S, Snyder SH (1999) Serine racemase: a glial enzyme synthesizing D-serine to regulate glutamate-*N*-methyl-D-aspartate neurotransmission. Proc Natl Acad Sci USA 96(23): 13409–13414. 10.1073/pnas.96.23.13409 [PubMed: 10557334]

Xu ZC, Wilson CJ, Emson PC (1989) Restoration of the corticostriatal projection in rat neostriatal grafts: electron microscopic analysis. Neuroscience 29(3):539–550 [PubMed: 2739900]

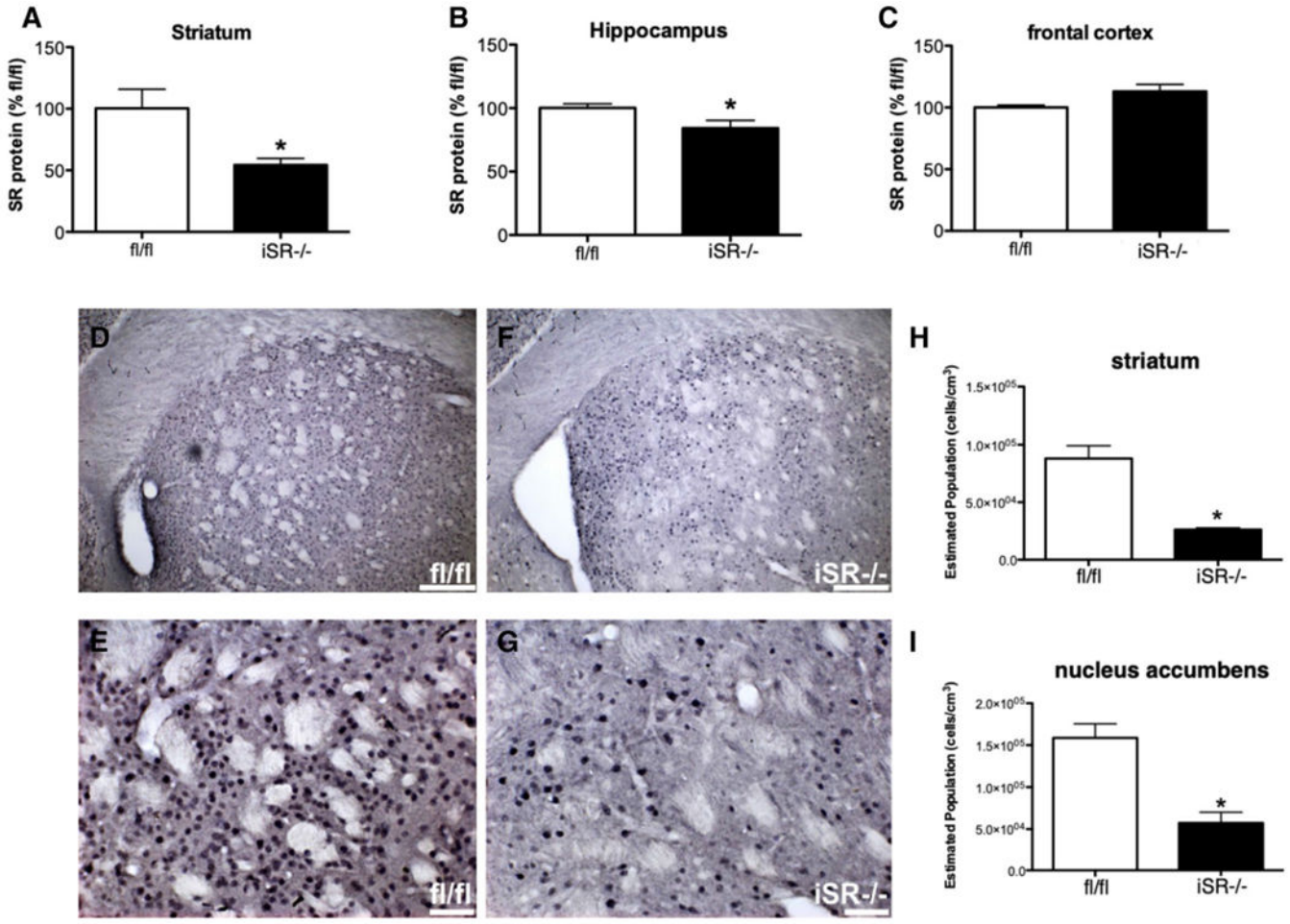

Fig. 1.

Western blot and cell counting showing SR reduction in striatum of iSR−/− mice. **a–c** Reduction of SR protein in iSR−/− mice. In iSR−/− mice, SR is reduced in striatum. There is no or very small reduction in hippocampus or frontal cortex. Protein levels of SR was measured in the striatum/hippocampus/frontal cortex of SRfl/fl mice ($n = 8$; white bars) and iSR−/− ($n = 8$; black bars) mice. Values are expressed as the optical density (OD) normalized to fl/fl mice. Asterisk indicates significant differences from the SRfl/fl mice ($p < 0.05$). **d–g** SR positive cells are sparse in iSR−/− mice (**f, g**) than SRfl/fl (**d, e**). White bars in **d** and **f** indicate 200 μm and in **e** and **g** indicate 40 μm. **h** and **i** SR reduction in striatum (**h**) and nucleus accumbens (**i**) of iSR−/− mice is confirmed by cell counting. Number of SR positive cells was counted in the striatum and nucleus accumbens of SRfl/fl ($n = 3$; white bars) and iSR−/− ($n = 3$; black bars) mice. Values are expressed as the estimated cell population (cells/cm^3). All values represent the mean ± SEM

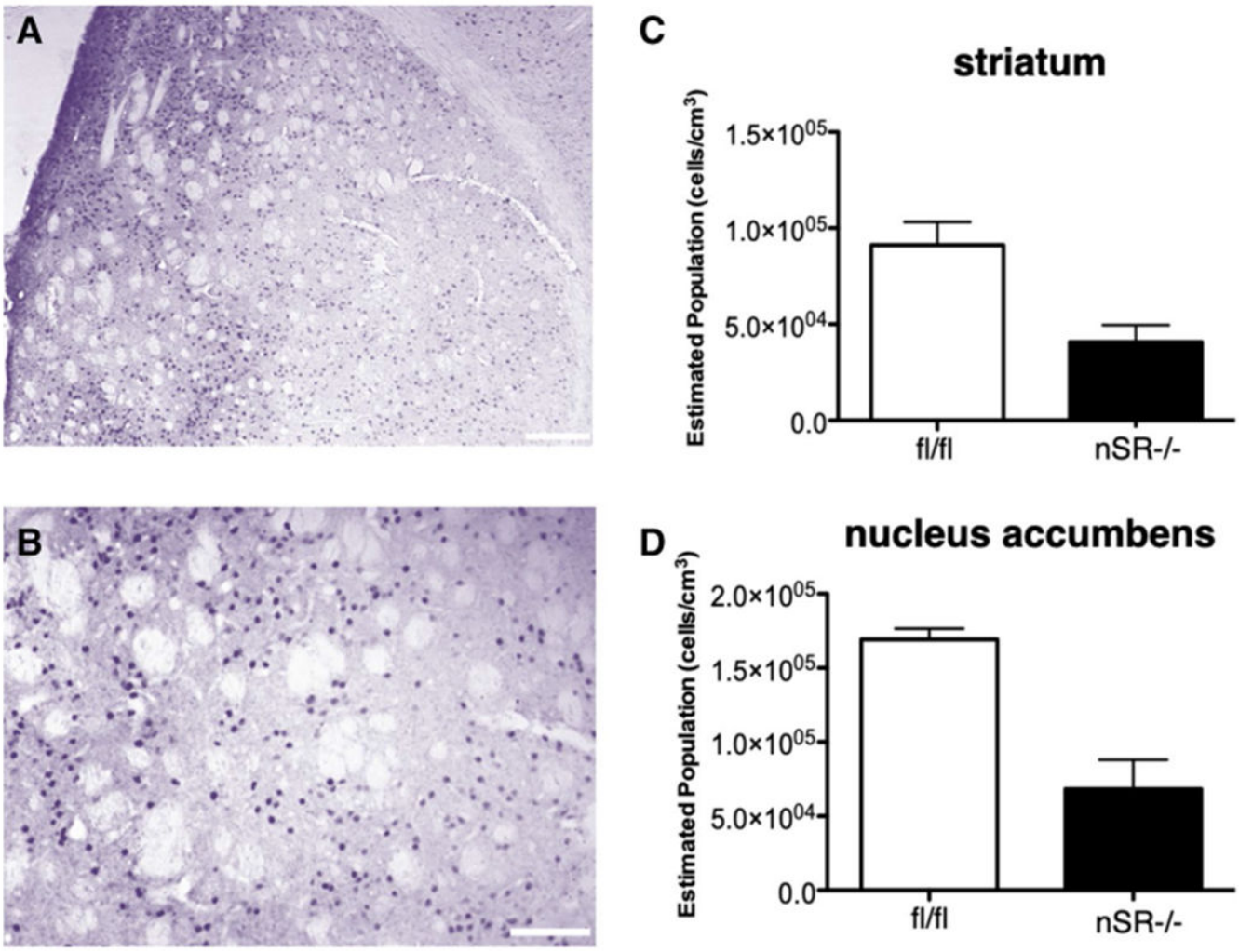

Fig. 2.

SR reduction in striatum of nSR−/− mice is similar to iSR−/−. **a** and **b** SR positive cells are as sparse in nSR−/− as in iSR−/− mice. White bar in **a** indicates 200 μm and in **b** indicates 40 μm. **c** and **d** SR reduction in striatum (**c**) and nucleus accumbens (**d**) of nSR−/− mice is confirmed by cell counting and it is similar to iSR−/− . The number of SR positive cells was counted in the striatum and nucleus accumbens of SRfl/fl (n = 3; white bars) and nSR−/− (n = 3; black bars) mice. Values are expressed as the estimated cell population (cells/cm^3). All values represent the mean ± SEM

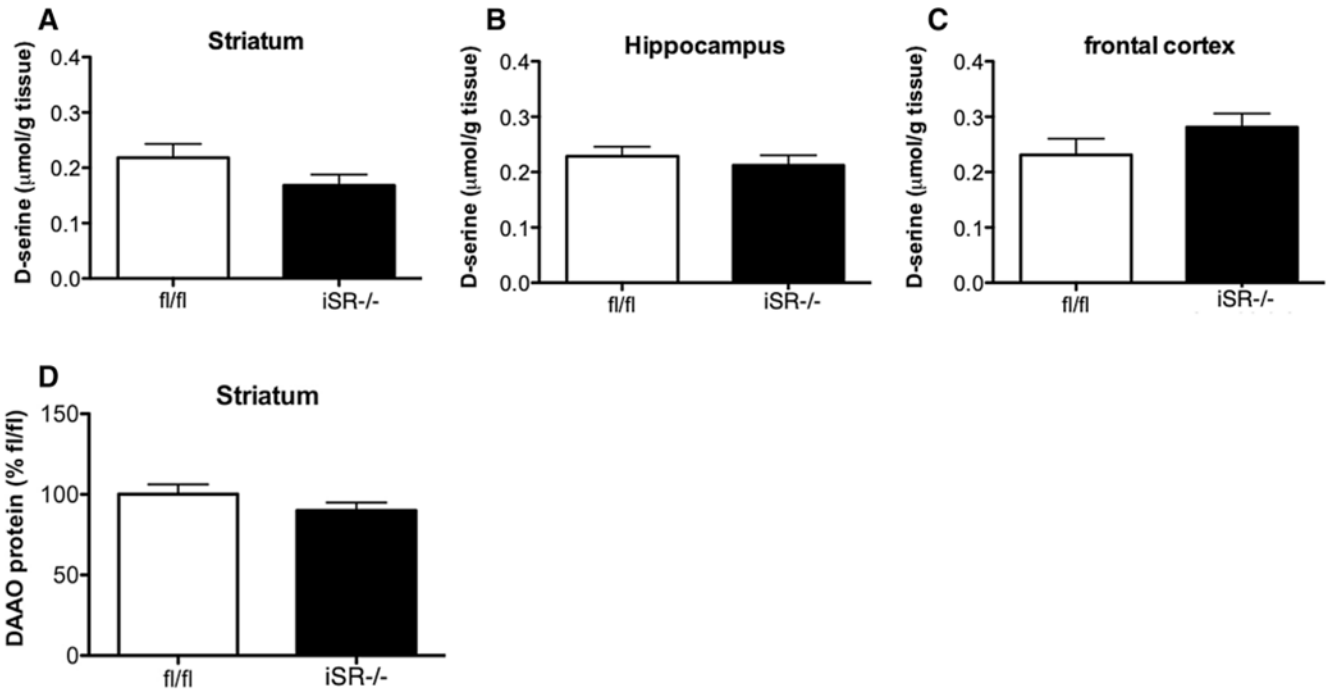

Fig. 3.

D-serine concentrations in the iSR−/− mice show only a small and statistically insignificant reductions in striatum and other areas. **a–c** HPLC was used to measure D-serine in iSR−/− and SRfl/fl mice. D-serine was measured in the striatum, hippocampus and frontal cortex of SRfl/fl ($n = 8$; white bars), iSR−/− mice ($n = 8$; black bars). Values are expressed as the μmol/g tissue. All values represent the mean ± SEM. **d** DAAO protein is not reduced in striatum of iSR−/− mice. Protein levels of DAAO were measured in the striatum of SRfl/fl ($n = 8$; white bars) and iSR−/− ($n = 8$; black bars) mice. Values are expressed as the optical density (OD) normalized to SRfl/fl

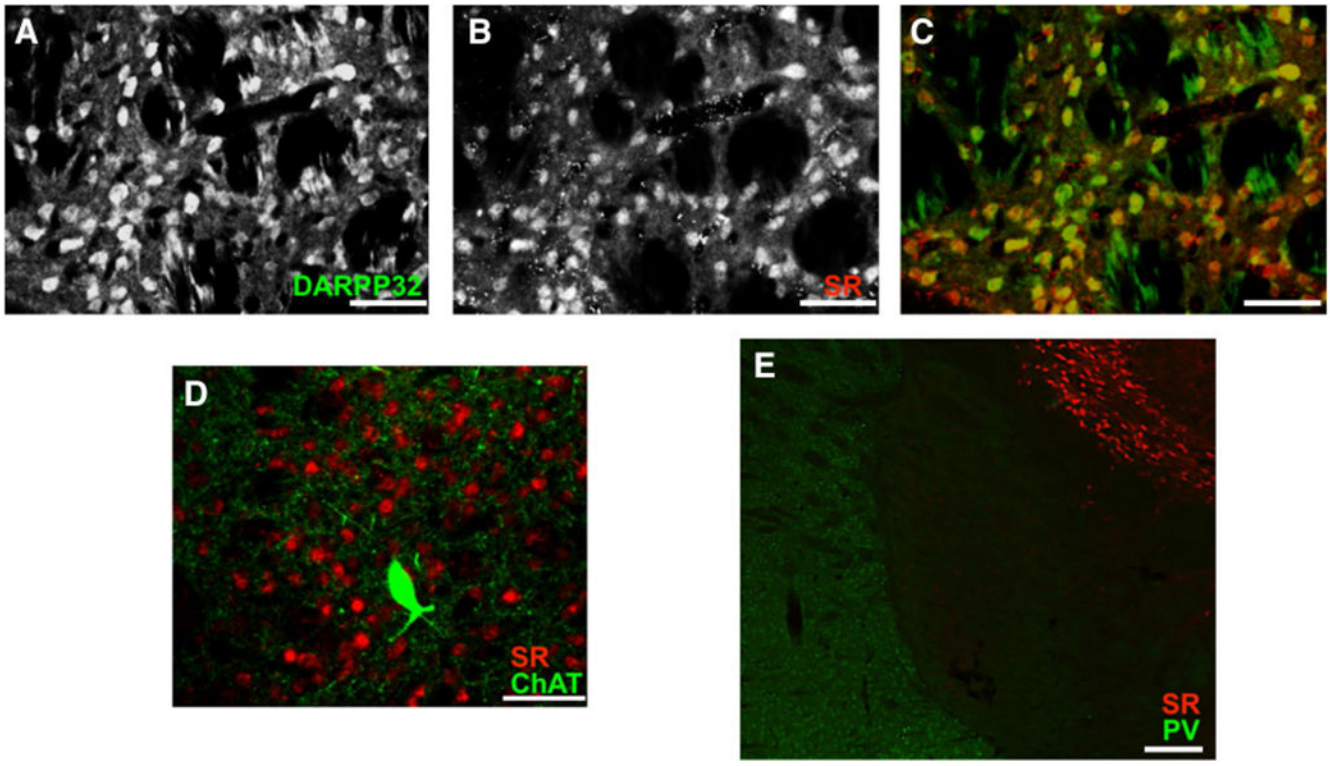

Fig. 4.

Medium spiny neurons express striatal SR; cholinergic and parvalbumin expressing neurons do not. **a–c** Robust co-localization of SR with DARPP32 is observed. White bars indicate 40 μm. **a** DARPP32, **b** SR, **c** merged figure of **a** and **b**. DARPP32 was shown in green fluorescence. SR was shown in red fluorescence. White bars indicate 40 μm. **d** Striatal cholinergic neurons do not co-express SR. ChAT is shown in green fluorescence. SR is shown in red fluorescence. White bars indicate 40 μm. **e** Fast-spiking interneurons do not co-express SR. Parvalbumin is shown in green fluorescence. SR is shown in red fluorescence. White bars indicate 200 μm

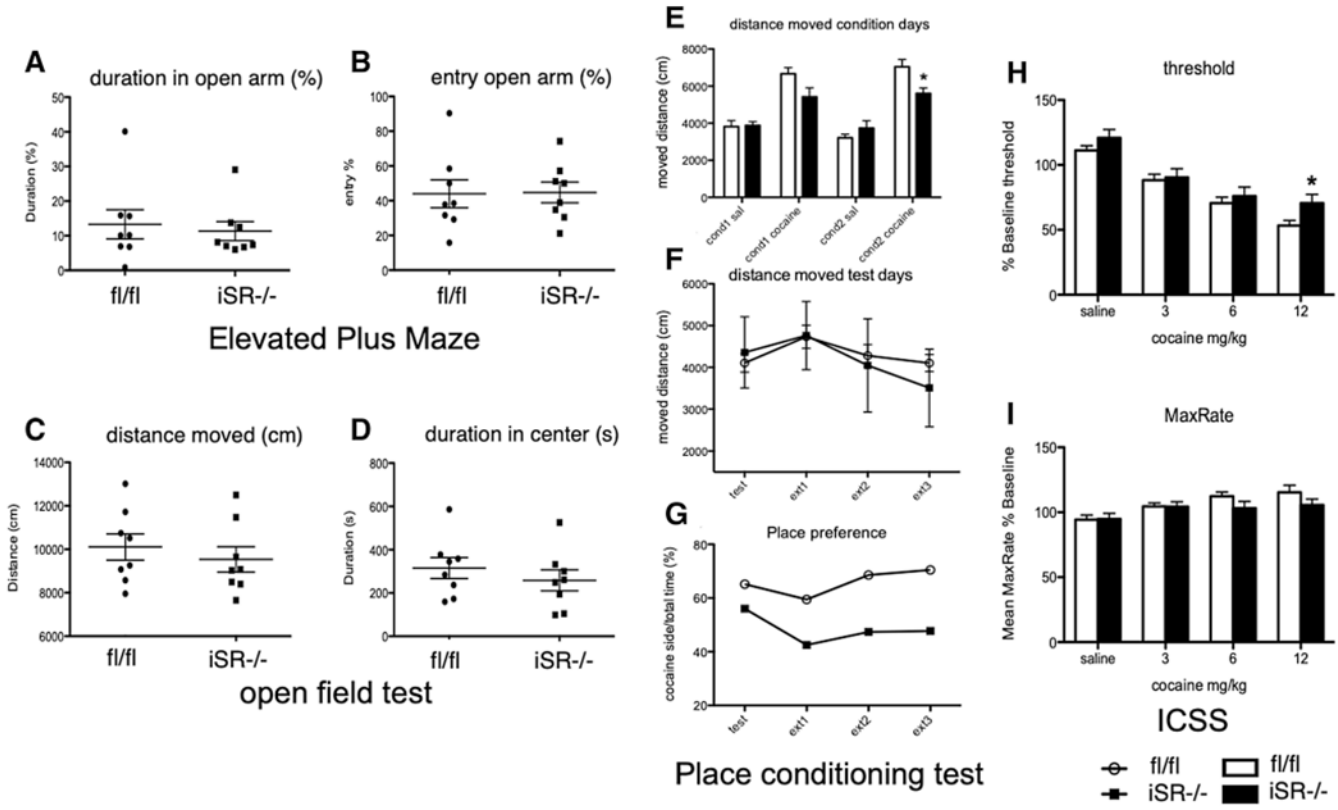

Fig. 5.

iSR−/− mice showed impaired sensitization to cocaine. **a** and **b** Elevated Plus Maze test shows no difference in anxiety between SRfl/fl (n = 8, black dots) and iSR−/− (n = 8, black squares). **a** The percentage of time that mice spent in the open arms in the total experiment time is shown. SRfl/fl do differ from iSR−/−. **b** The percentage of the number of entries in open arms in the number of entries in both open and closed arms is shown. SRfl/fl do not differ from iSR−/−. **c** and **d** Open field test shows no difference in anxiety between SRfl/fl (n = 8, black dots) and iSR−/− mice (n = 8, black square). **c** The distance travelled by mice during the experiment time is not different between SRfl/fl (n = 8, black dots) and iSR−/− mice (n = 8, black square). **d** The time spent in the center zone by mice during the experiment time is not different between SRfl/fl (n = 8, black dots) and iSR−/− mice (n = 8, black squares). **e–g** The place conditioning task with cocaine shows less cocaine locomotor sensitization for iSR−/− mice, which do not maintain a preference for the cocaine chamber on extinction days. **e** On the conditioning days, iSR−/− mice (n = 9, black bars) travel significantly less distance on second conditioning day than SRfl/fl mice (n = 9, white bars, p = 0.010). **f** There is no difference in the distance travelled on test day and extension days between iSR−/− (black squares) and SRfl/fl mice (white dots). **g** At the test day, both iSR−/− mice (n = 9, black squares) and SRfl/fl (n = 9, white dots). show a significant preference for the cocaine chamber (0.05). However, iSR−/− mice do not show a significant preference for the cocaine chamber on the subsequent extinction days whereas SRfl/fl maintained significant preference for the cocaine chamber (p = 0.014, 0.001, 0.001, respectively). **h** and **i** iSR−/− mice react less in ICSS threshold following cocaine administration. h ICSS

thresholds showed significant main effect of cocaine dose (F=46.756, p < 2e–16) and close to significant main effects of genotype (F = 3.803, p = 0.0522). A t-test for the result at 12 mg/kg showed significant p value (p = 0.022). iSR−/− (n = 5, black bars), SRfl/fl (n = 7, white bars). **i** ICSS maximum response rates show significant main effects of cocaine dose (F = 5.429, p = 0.0012). Although a tendency for less dependent response to cocaine dose in iSR−/− mice (black bars) than in fl/fl mice (white bars) is confirmed, the main effect of genotype was not found to be significant

Table 1

SR co-localization with D1 and D2 dopamine receptors in striatum

	SR cell count	DR cell count	% DR cells in SR	% SR cells in D1/D2R
D1-tdTomato	892	314	100	37
D2-tdTomato	426	280	100	66

Reporter mice with tdTomato transgene expressed by either D1 or D2 dopamine receptors showed complete co-expression with SR in immunofluorescent-stained slices. Cells were counted using Stereo Investigator stereology software for unbiased random sampling throughout the striatum. The results the total number of cells ascertained from three sections from three mice

DR dopamine receptor